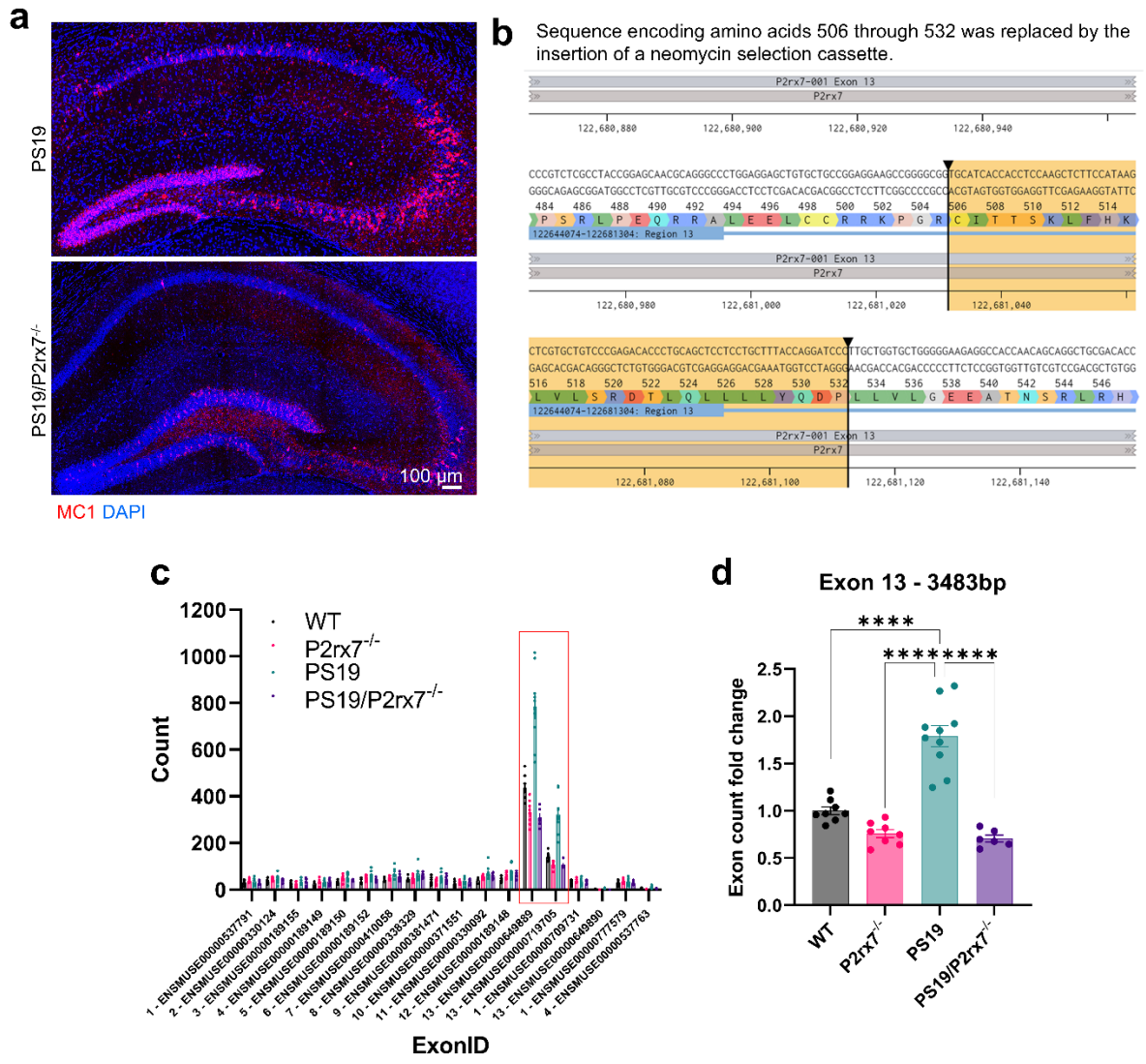

Extended Data Fig. 1: *P2rx7* deficiency regulation of misfolded tau accumulation and *P2rx7* transcripts in hippocampus of 9.5-month-old PS19 mice. a, Representative confocal images of misfolded tau (MC1 antibody) staining in hippocampus from PS19 and PS19/P2rx7$^{-/-}$ mice. **b,** Sequence encoding amino acids 506 through 532 was replaced by the insertion of a neomycin selection cassette in P2rx7$^{-/-}$ mice created by Pfizer. **c**, *P2rx7* exon transcripts count in hippocampus from 9.5-month-old mice (*n*= 8

WT mice, *n*= 8 P2rx7$^{-/-}$ mice, *n*= 10 PS19 mice, *n*= 6 PS19/P2rx7$^{-/-}$). **d**, Expression levels of *P2rx7* exon 13 transcripts (*n*= 8 WT mice, *n*= 8 P2rx7$^{-/-}$ mice, *n*= 10 PS19 mice, *n*= 6 PS19/P2rx7$^{-/-}$ mice). All the bar graphs are represented by mean ± SEM; ****$P < 0.0001$ by one-way ANOVA with Holm–Šidák post hoc analysis.

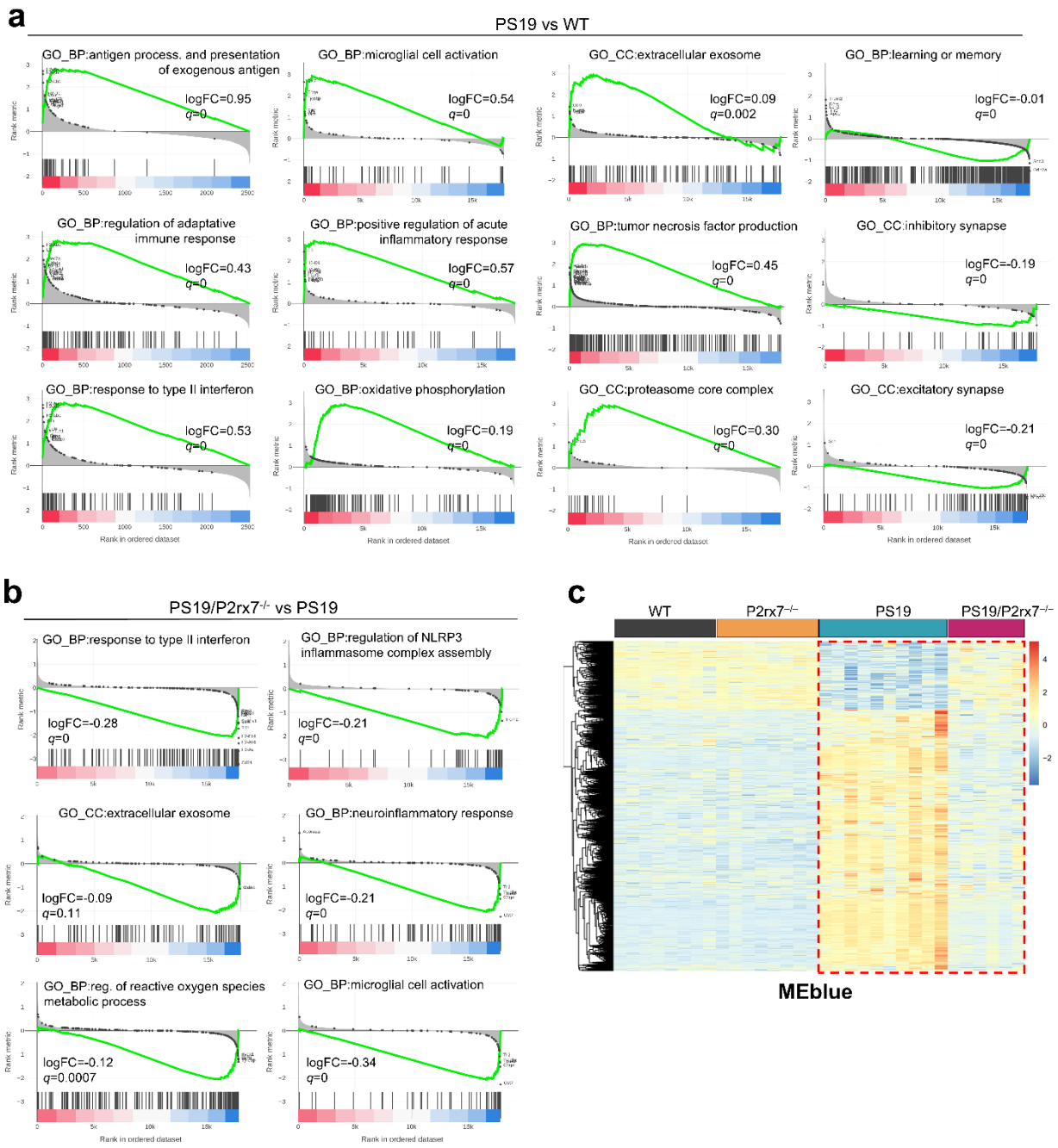
a
PS19 vs WT
GO_BP:antigen process. and presentation of exogenous antigen
logFC=0.95
q=0
GO_BP:microglial cell activation
logFC=0.54
q=0
GO_CC:extracellular exosome
logFC=0.09
q=0.002
GO_BP:learning or memory
logFC=-0.01
q=0
GO_BP:regulation of adaptative immune response
logFC=0.43
q=0
GO_BP:positive regulation of acute inflammatory response
logFC=0.57
q=0
GO_BP:tumor necrosis factor production
logFC=0.45
q=0
GO_CC:inhibitory synapse
logFC=-0.19
q=0
GO_BP:response to type II interferon
logFC=0.53
q=0
GO_BP:oxidative phosphorylation
logFC=0.19
q=0
GO_CC:proteasome core complex
logFC=0.30
q=0
GO_CC:excitatory synapse
logFC=-0.21
q=0
Rank metric
Rank in ordered dataset
b
PS19/P2rx7-/- vs PS19
GO_BP:response to type II interferon
logFC=-0.28
q=0
GO_BP:regulation of NLRP3 inflammasome complex assembly
logFC=-0.21
q=0
GO_CC:extracellular exosome
logFC=-0.09
q=0.11
GO_BP:neuroinflammatory response
logFC=-0.21
q=0
GO_BP:reg. of reactive oxygen species metabolic process
logFC=-0.12
q=0.0007
GO_BP:microglial cell activation
logFC=-0.34
q=0
Rank metric
Rank in ordered dataset
c
WT
P2rx7-/-
PS19
PS19/P2rx7-/-
MEblue
d
GO: extracellular exosome/exosome biogenesis
z-score
WT
P2rx7-/-
PS19
PS19/P2rx7-/-

Extended Data Fig. 2: **Bulk RNA-seq of PS19 mouse hippocampus. a-b**, Gene set enrichment analysis (GSEA) of top pathways regulated in bulk RNA-seq of hippocampus from PS19 versus WT (a) and PS19/P2rx7$^{-/-}$ versus PS19 (b) mice (*n*= 10 PS19 mice, *n*= 6 PS19/P2rx7$^{-/-}$ mice). **c**, Heatmap comparing the gene expression levels from module MEblue among the groups. PS19 and PS19/P2rx7$^{-/-}$ mice groups are highlighted with dashed lines (*n*= 8 WT mice, *n*= 8 P2rx7$^{-/-}$ mice, *n*= 10 PS19 mice and *n*= 6 PS19/P2rx7$^{-/-}$ mice). **d**, Heatmap displaying the expression level of genes associated with extracellular vesicles/extracellular exosome and exosome biogenesis gene ontology (GO) pathways (*n*= 8 WT mice, *n*= 8 P2rx7$^{-/-}$ mice, *n*= 10 PS19 mice, *n*= 6 PS19/P2rx7$^{-/-}$ mice).

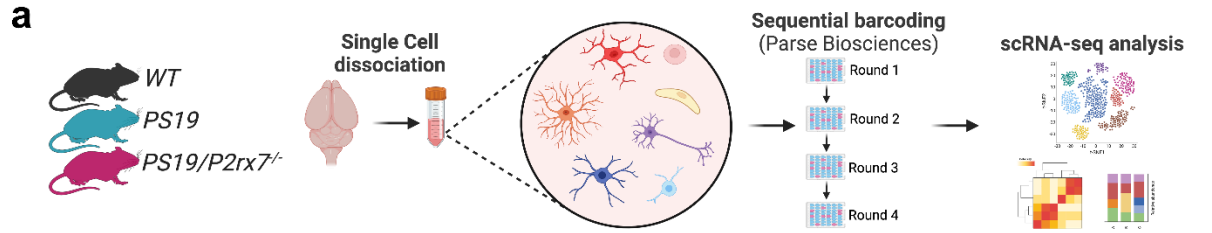
a
WT
PS19
PS19/P2rx7-/-
Single Cell dissociation
Sequential barcoding (Parse Biosciences)
Round 1
Round 2
Round 3
Round 4
scRNA-seq analysis

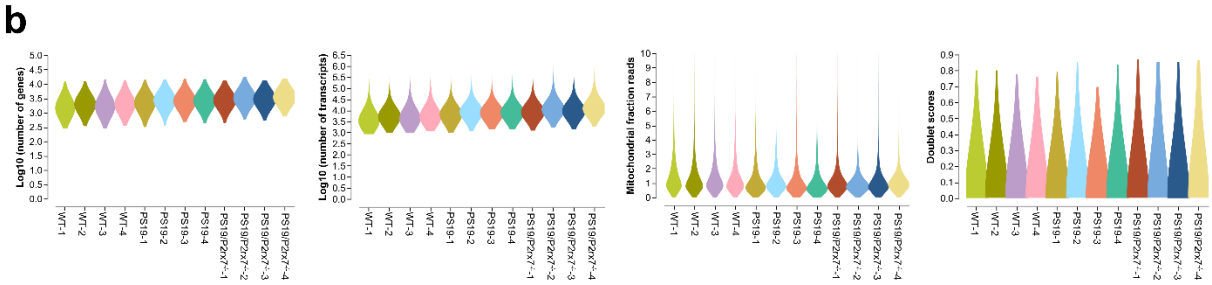
b
Log10 (number of genes)
Log10 (number of transcripts)
Mitochondrial fraction reads
Doublet scores
WT-1
WT-2
WT-3
WT-4
PS19-1
PS19-2
PS19-3
PS19-4
PS19/P2rx7-/--1
PS19/P2rx7-/--2
PS19/P2rx7-/--3
PS19/P2rx7-/--4

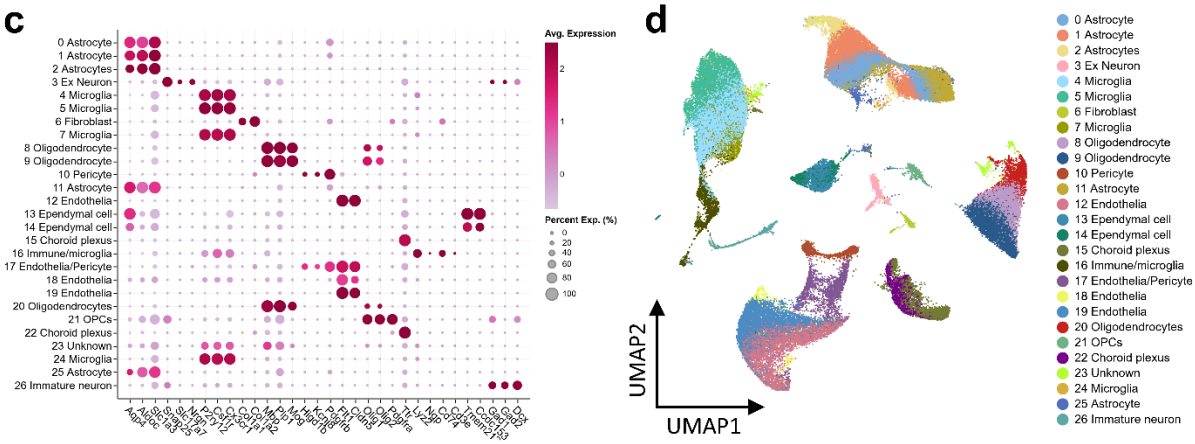
c
0 Astrocyte
1 Astrocyte
2 Astrocytes
3 Ex Neuron
4 Microglia
5 Microglia
6 Fibroblast
7 Microglia
8 Oligodendrocyte
9 Oligodendrocyte
10 Pericyte
11 Astrocyte
12 Endothelia
13 Ependymal cell
14 Ependymal cell
15 Choroid plexus
16 Immune/microglia
17 Endothelia/Pericyte
18 Endothelia
19 Endothelia
20 Oligodendrocytes
21 OPCs
22 Choroid plexus
23 Unknown
24 Microglia
25 Astrocyte
26 Immune neuron
Avg. Expression
Percent Exp. (%)
d
UMAP2
UMAP1

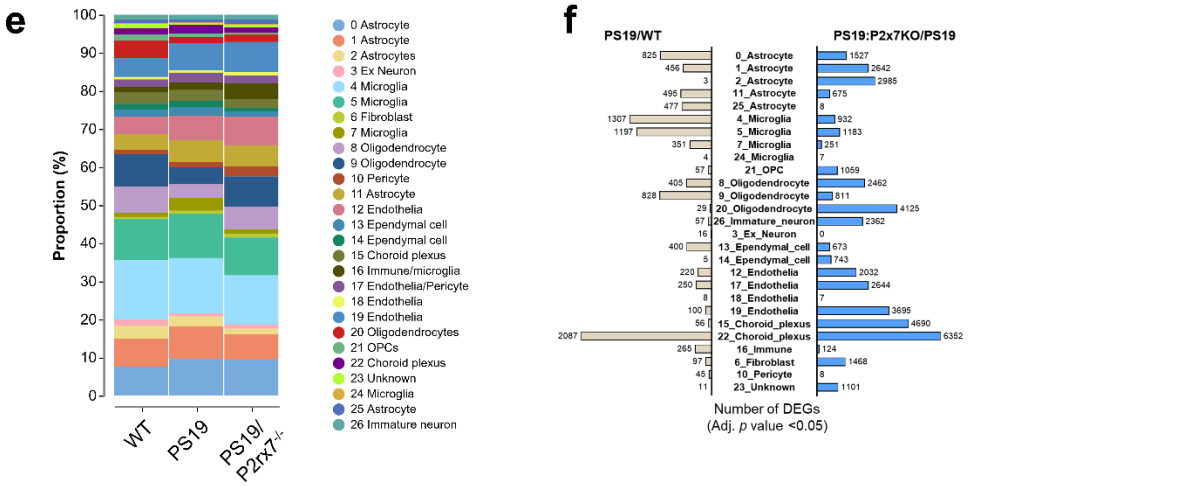
e
Proportion (%)
WT
PS19
PS19/ P2rx7-/-
f
PS19/WT
PS19:P2x7KO/PS19
Number of DEGs
(Adj. p value <0.05)

Extended Data Fig. 3: scRNA-seq of PS19 mouse brain cells. a, Schematic design for scRNA-seq analysis of hippocampus from 9.5-month-old mice (*n*= 4 mice per group). **b**, Quality control measures in scRNA-seq analysis of mouse brain cells showing the number of genes, transcripts, mitochondrial fraction reads and doublets scores per each sample (*n*= 4 mice per group). **c**, Dot-plot depicting normalized average expression of selected genes used for cell identity annotation for each of 27 identified cell clusters. **d**, UMAP representation of 27 clusters identified in scRNA-seq analysis of 89,795 cells from brain cortex from WT, PS19 and PS19/P2rx7$^{-/-}$ mice. **e**, Stacked barplot showing the cell cluster compositions from WT, PS19 and PS19/P2rx7$^{-/-}$ mouse brains. Cluster annotation indicated by colors shown in c. **f**, Number of differentially expressed genes per cell cluster in PS19 versus WT and PS19/P2rx7$^{-/-}$ versus PS19 mice (*n*= 4 per group, $P < 0.05$).

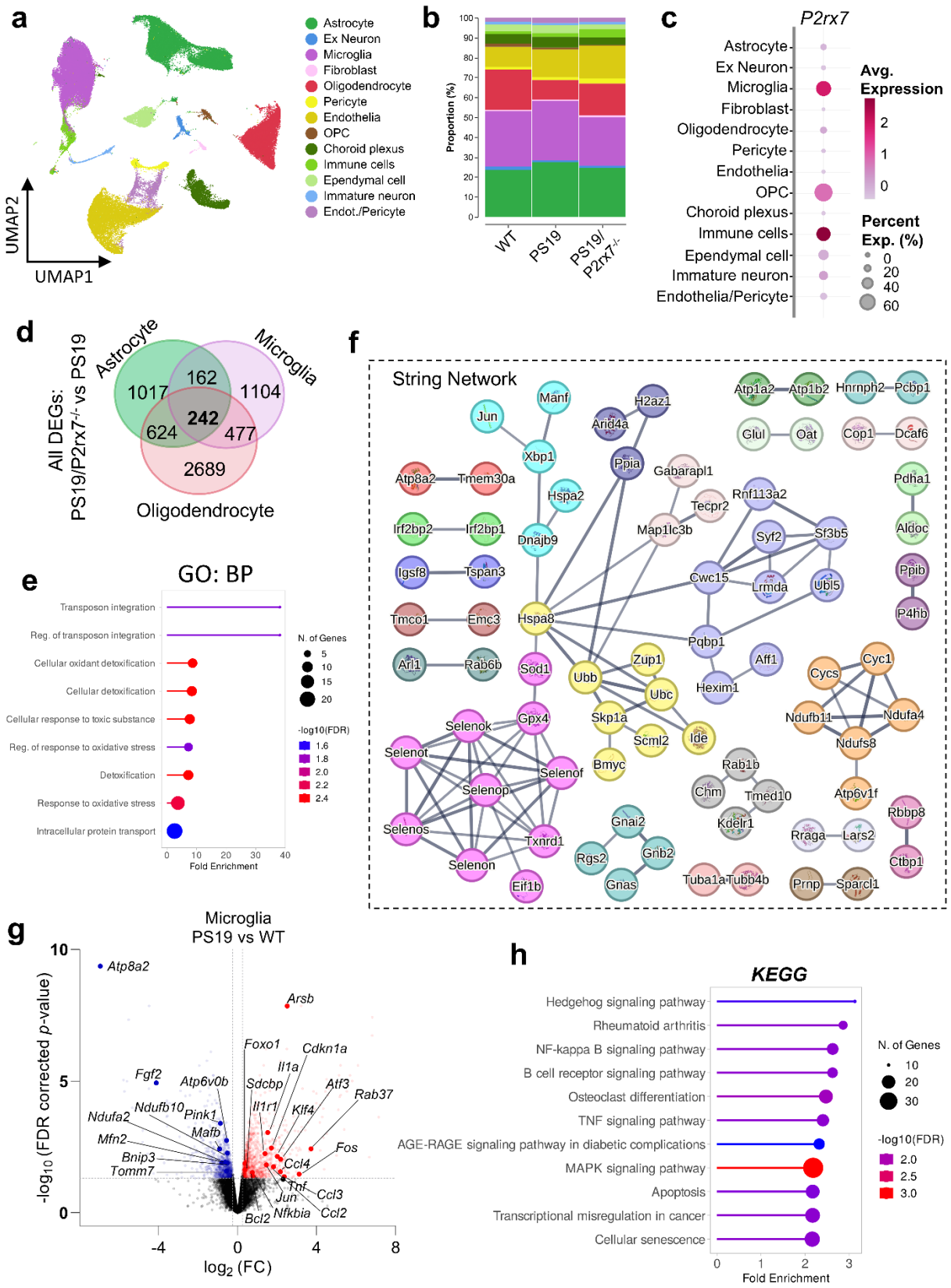
a
UMAP2
UMAP1
Astrocyte
Ex Neuron
Microglia
Fibroblast
Oligodendrocyte
Pericyte
Endothelia
OPC
Choroid plexus
Immune cells
Ependymal cell
Immature neuron
Endot./Pericyte
b
Proportion (%)
WT
PS19
PS19/P2rx7-/-
c
P2rx7
Astrocyte
Ex Neuron
Microglia
Fibroblast
Oligodendrocyte
Pericyte
Endothelia
OPC
Choroid plexus
Immune cells
Ependymal cell
Immature neuron
Endothelia/Pericyte
Avg. Expression
Percent Exp. (%)
d
All DEGs: PS19/P2rx7-/- vs PS19
Astrocyte
Microglia
Oligodendrocyte
1017
162
1104
242
624
477
2689
e
GO: BP
Transposon integration
Reg. of transposon integration
Cellular oxidant detoxification
Cellular detoxification
Cellular response to toxic substance
Reg. of response to oxidative stress
Detoxification
Response to oxidative stress
Intracellular protein transport
N. of Genes
-log10(FDR)
Fold Enrichment
f
String Network
g
Microglia
PS19 vs WT
-log10 (FDR corrected p-value)
log2 (FC)
h
KEGG
Hedgehog signaling pathway
Rheumatoid arthritis
NF-kappa B signaling pathway
B cell receptor signaling pathway
Osteoclast differentiation
TNF signaling pathway
AGE-RAGE signaling pathway in diabetic complications
MAPK signaling pathway
Apoptosis
Transcriptional misregulation in cancer
Cellular senescence
N. of Genes
-log10(FDR)
Fold Enrichment

Extended Data Fig. 4: scRNA-seq reveals distinct effects of *P2rx7* deficiency on glial populations in PS19 mouse brain. a, UMAP representation of scRNA-seq analysis of 89,795 cells from brain cortex from WT, PS19 and PS19/P2rx7$^{-/-}$ mice grouped by major cell type. **b**, Stacked bar plot showing the cell-type compositions from WT, PS19 and PS19/P2rx7$^{-/-}$ mouse brains. **c**, Dot-plot showing normalized average expression levels of *P2rx7* gene in different cell types. **d**, Volcano plot showing differentially expressed genes in all microglia cells from PS19 versus WT mice (n= 4 mice per group, $P < 0.05$). **e**, Top enriched GO annotations of differentially expressed genes upregulated in microglia from PS19 vs WT mice (n= 4 mice per group, $P < 0.05$). **f**, Vein diagram showing differentially expressed genes regulated by P2rx7 deletion in PS19 mice overlapped among glial cells ($P < 0.05$ and log2FC > ±0.25). **g**, Top enriched GO biological process (BP) annotations of 242 differentially expressed genes commonly regulated by P2rx7 deletion in glial cells from PS19 mice. **h**, String gene network of commonly regulated genes by P2rx7 deletion in glial cells from PS19 mice filtered by interaction confidence.

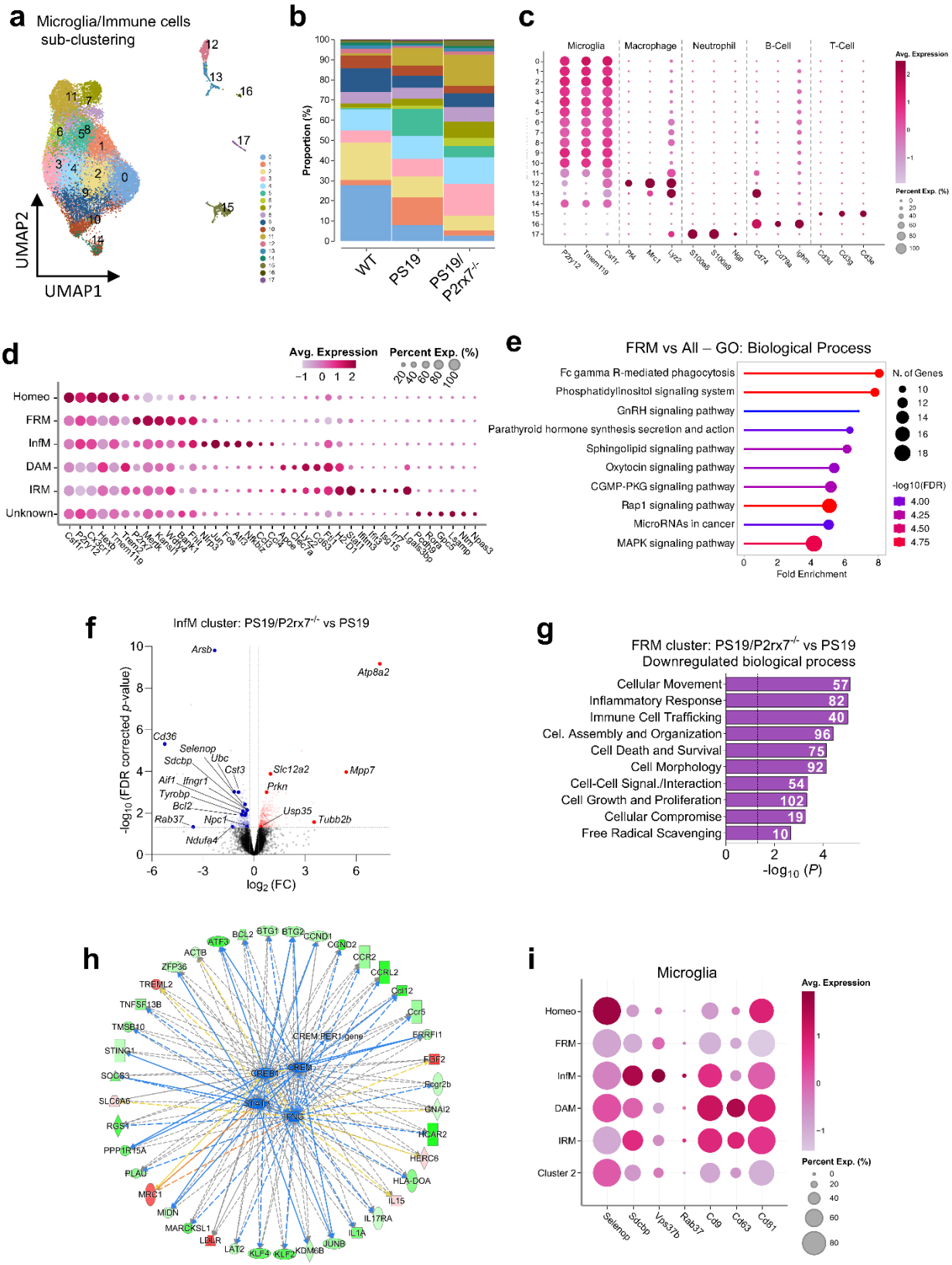
a
Microglia/Immune cells sub-clustering
UMAP1
UMAP2
b
Proportion (%)
WT
PS19
PS19/ P2rx7-/-
c
Microglia
Macrophage
Neutrophil
B-Cell
T-Cell
Avg. Expression
Percent Exp. (%)
d
Avg. Expression
Percent Exp. (%)
Homeo
FRM
InfM
DAM
IRM
Unknown
e
FRM vs All – GO: Biological Process
Fc gamma R-mediated phagocytosis
Phosphatidylinositol signaling system
GnRH signaling pathway
Parathyroid hormone synthesis secretion and action
Sphingolipid signaling pathway
Oxytocin signaling pathway
CGMP-PKG signaling pathway
Rap1 signaling pathway
MicroRNAs in cancer
MAPK signaling pathway
N. of Genes
-log10(FDR)
Fold Enrichment
f
InfM cluster: PS19/P2rx7-/- vs PS19
-log10 (FDR corrected p-value)
log2 (FC)
g
FRM cluster: PS19/P2rx7-/- vs PS19
Downregulated biological process
Cellular Movement
Inflammatory Response
Immune Cell Trafficking
Cel. Assembly and Organization
Cell Death and Survival
Cell Morphology
Cell-Cell Signal./Interaction
Cell Growth and Proliferation
Cellular Compromise
Free Radical Scavenging
-log10 (P)
h
i
Microglia
Homeo
FRM
InfM
DAM
IRM
Cluster 2
Avg. Expression
Percent Exp. (%)

Extended Data Fig. 5: Sub clustering of microglia and immune cells in scRNA-seq. **a**, UMAP plots representation of 26,801 microglia and immune cells distributed in 18 subclusters (*n*=4 mice per group). **b**, Stacked barplot showing the compositions of microglia and immune cells subcluster in WT, PS19 and PS19/P2rx7$^{-/-}$. **c**, Dot-plot depicting normalized average expression of selected genes used for cell identity annotation and filtering immune cells clusters. **d**, Dot-plot showing normalized average expression of selected genes used for microglia state annotation in filtered microglia cell population. **e**, Top enriched GO annotations of differentially expressed genes enriched in microglia FRM in comparison with all other microglia clusters. **f**, Volcano plot showing DEGs regulated in InfM cluster from PS19/P2rx7$^{-/-}$ mice. **g**, Ingenuity pathway analysis (IPA) of biological process annotations downregulated in FRM cluster from PS19/P2rx7$^{-/-}$ mice. **h**, Gene interaction network and master regulators in FRM cluster from PS19/P2rx7$^{-/-}$ mice predicted by IPA. **i**, Dot-plot showing normalized average expression of selected genes associated with EV secretion in different microglia states from scRNA-seq data.

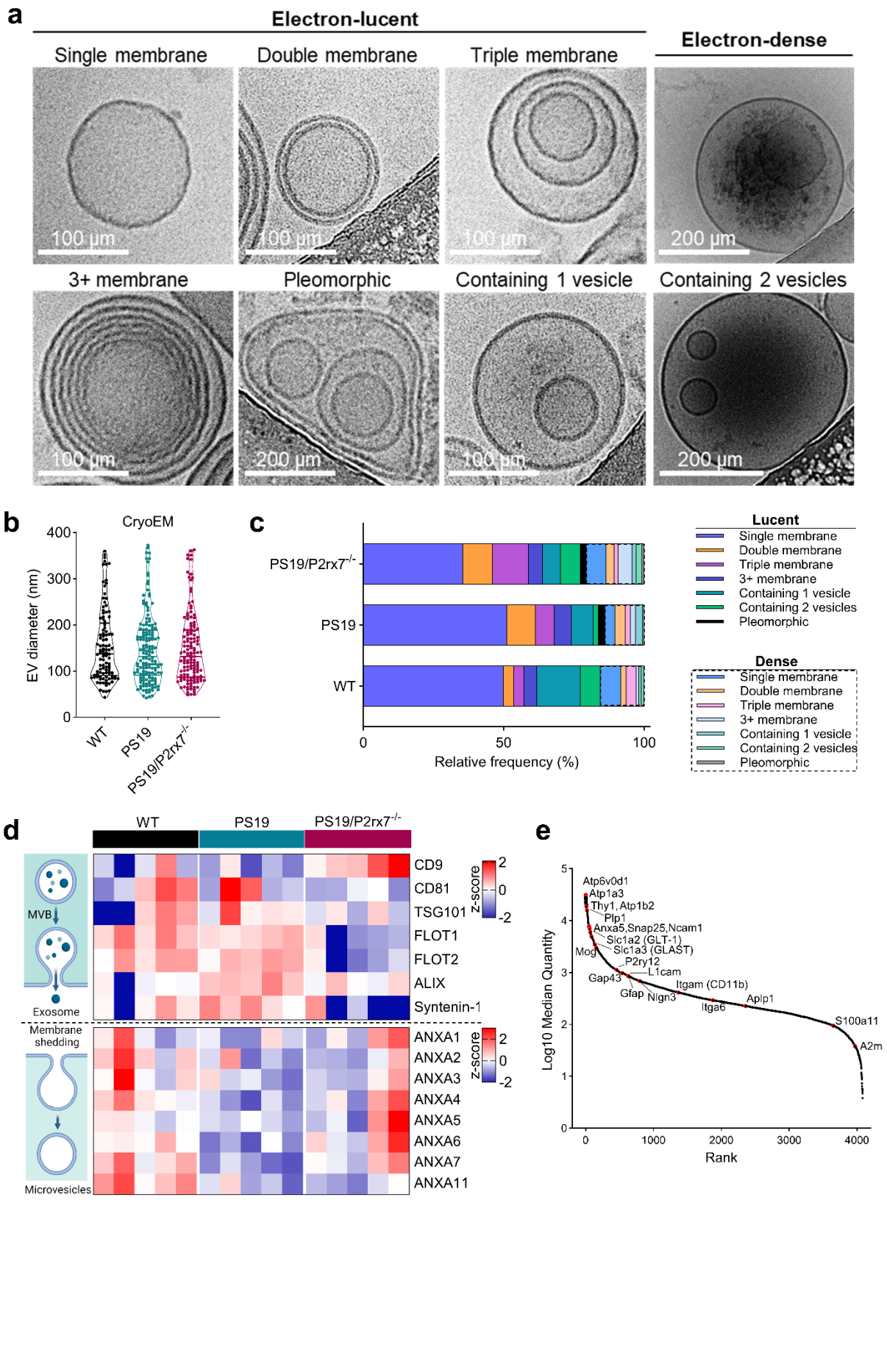
a
Electron-lucent
Electron-dense
Single membrane
Double membrane
Triple membrane
3+ membrane
Pleomorphic
Containing 1 vesicle
Containing 2 vesicles
100 µm
200 µm
b
CryoEM
EV diameter (nm)
WT
PS19
PS19/P2rx7-/-
c
Relative frequency (%)
Lucent
Dense
d
MVB
Exosome
Membrane shedding
Microvesicles
CD9
CD81
TSG101
FLOT1
FLOT2
ALIX
Syntenin-1
ANXA1
ANXA2
ANXA3
ANXA4
ANXA5
ANXA6
ANXA7
ANXA11
z-score
e
Log10 Median Quantity
Rank
Atp6v0d1
Atp1a3
Thy1, Atp1b2
Plp1
Anxa5,Snap25,Ncam1
Slc1a2 (GLT-1)
Slc1a3 (GLAST)
Mog
P2ry12
L1cam
Gap43
Itgam (CD11b)
Gfap
Nlgn3
Itga6
Aplp1
S100a11
A2m

Extended Data Fig. 6: DIA mass spectrometry and cryo-EM analysis of mouse BDEVs. a-c, Cryo-EM analysis of size (**a**,**b**), morphology and electron density (**a**,**c**) of BDEVs isolated from 9.5-month-old mouse brain (*n*= 3 mice per group; total BDEVs analyzed *n*= 105 WT, 156 PS19 and 135 PS19/P2rx7$^{-/-}$). **d**, Heatmap showing the expression level of exosome and microvesicles proteins in BDEVs (*n*= 5 mice per group). **e**, Protein rank displaying selected cell-type specific proteins found in BDEVs (*n*= 5 mice per group).

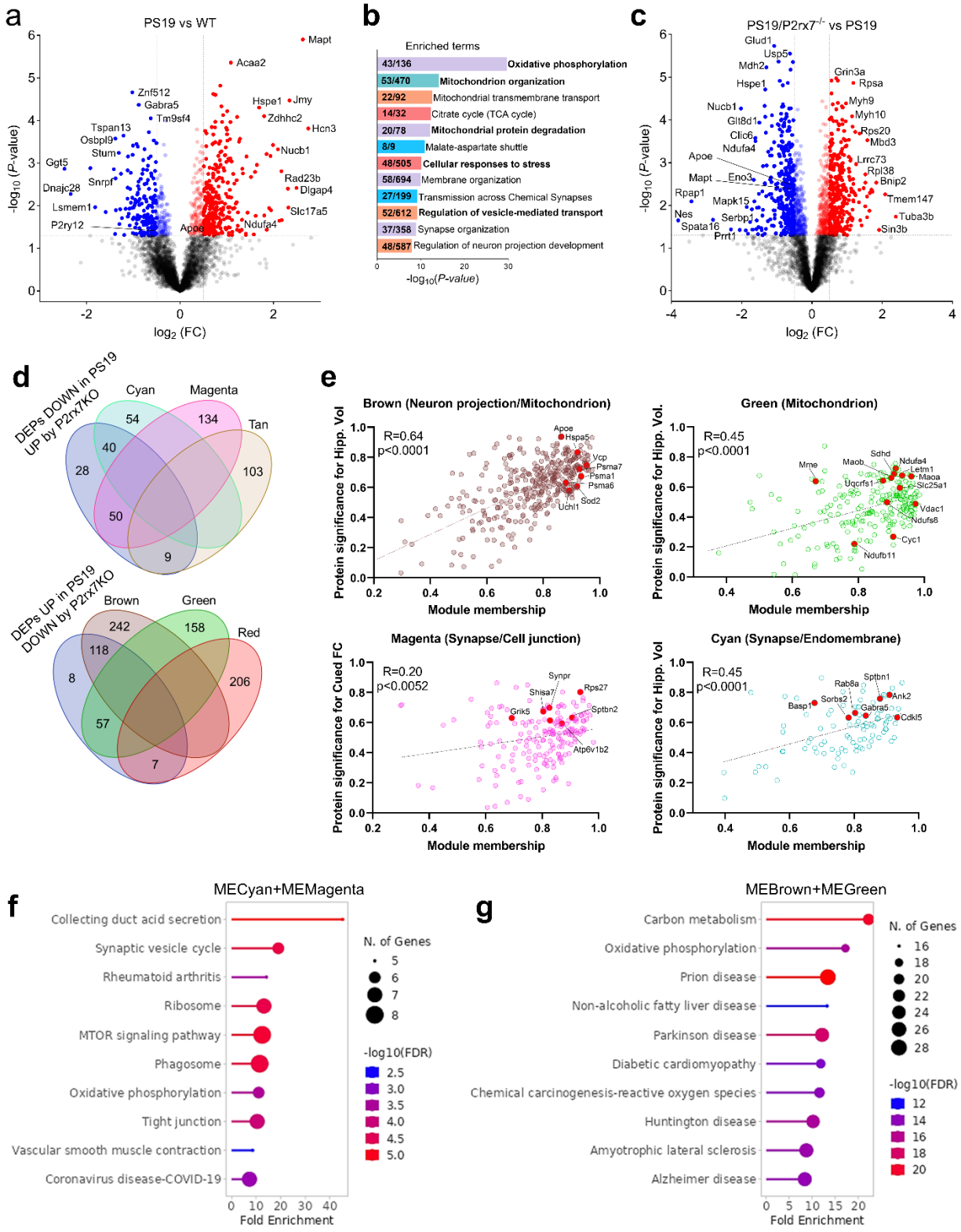
a
PS19 vs WT
-log10 (P-value)
log2 (FC)
Mapt
Acaa2
Znf512
Gabra5
Tm9sf4
Hspe1
Jmy
Zdhhc2
Hcn3
Tspan13
Osbpl9
Stum
Nucb1
Ggt5
Snrpf
Rad23b
Dnajc28
Dlgap4
Lsmem1
Slc17a5
P2ry12
Apoe
Ndufa4
b
Enriched terms
43/136 Oxidative phosphorylation
53/470 Mitochondrion organization
22/92 Mitochondrial transmembrane transport
14/32 Citrate cycle (TCA cycle)
20/78 Mitochondrial protein degradation
8/9 Malate-aspartate shuttle
48/505 Cellular responses to stress
58/694 Membrane organization
27/199 Transmission across Chemical Synapses
52/612 Regulation of vesicle-mediated transport
37/358 Synapse organization
48/587 Regulation of neuron projection development
-log10(P-value)
c
PS19/P2rx7-/- vs PS19
-log10 (P-value)
log2 (FC)
Glud1
Usp5
Mdh2
Grin3a
Rpsa
Hspe1
Myh9
Nucb1
Myh10
Glt8d1
Rps20
Clic6
Mbd3
Ndufa4
Apoe
Lrrc73
Mapt
Eno3
Rpl38
Bnip2
Rpap1
Mapk15
Tmem147
Nes
Serbp1
Tuba3b
Spata16
Prrt1
Sin3b
d
DEPs DOWN in PS19
UP by P2rx7KO
Cyan
Magenta
Tan
54
134
40
28
103
50
9
DEPs UP in PS19
DOWN by P2rx7KO
Brown
Green
Red
242
158
118
8
206
57
7
e
Brown (Neuron projection/Mitochondrion)
R=0.64
p<0.0001
Protein significance for Hipp. Vol
Module membership
Apoe
Hspa5
Vcp
Psma7
Psma1
Psma6
Sod2
Uchl1
Green (Mitochondrion)
R=0.45
p<0.0001
Mme
Maob
Sdhd
Ndufa4
Letm1
Maoa
Ugcrfs1
Slc25a1
Vdac1
Ndufs8
Cyc1
Ndufb11
Magenta (Synapse/Cell junction)
R=0.20
p<0.0052
Protein significance for Cued FC
Synpr
Rps27
Shisa7
Grik5
Sptbn2
Atp6v1b2
Cyan (Synapse/Endomembrane)
R=0.45
p<0.0001
Sptbn1
Rab8a
Ank2
Sorbs2
Basp1
Gabra5
Cdkl5
f
MECyan+MEMagenta
Collecting duct acid secretion
Synaptic vesicle cycle
Rheumatoid arthritis
Ribosome
MTOR signaling pathway
Phagosome
Oxidative phosphorylation
Tight junction
Vascular smooth muscle contraction
Coronavirus disease-COVID-19
Fold Enrichment
N. of Genes
5
6
7
8
-log10(FDR)
2.5
3.0
3.5
4.0
4.5
5.0
g
MEBrown+MEGreen
Carbon metabolism
Oxidative phosphorylation
Prion disease
Non-alcoholic fatty liver disease
Parkinson disease
Diabetic cardiomyopathy
Chemical carcinogenesis-reactive oxygen species
Huntington disease
Amyotrophic lateral sclerosis
Alzheimer disease
Fold Enrichment
N. of Genes
16
18
20
22
24
26
28
-log10(FDR)
12
14
16
18
20

Extended Data Fig. 7: Brain-EV proteomics and co-expression network analysis shows the key molecular signature associated with disease amelioration in *P2rx7*-deficient PS19 mice. a, Volcano plot of DIA mass spectrometry showing differentially expressed protein (DEPs) in BDEVs from PS19 versus WT mice (n=5 mice per group, $P < 0.05$). **b**, Enriched pathway terms of DEPs upregulated in PS19 versus WT mice comparison. **c**, Volcano plot showing DEPs in BDEVs from PS19/P2rx7$^{-/-}$ versus PS19 mice (n=5 mice per group, $P < 0.05$). **d,** Venn diagram showing the protein modules overlap with DEPs regulated in PS19 mice by P2rx7KO. **e,** Correlation analysis of protein significance and modular enrichment with disease phenotype. Main proteins regulated by *P2rx7* deficiency were highlighted in red. **f,g**, GO-KEGG analysis of the main overlapped modules from **d**.

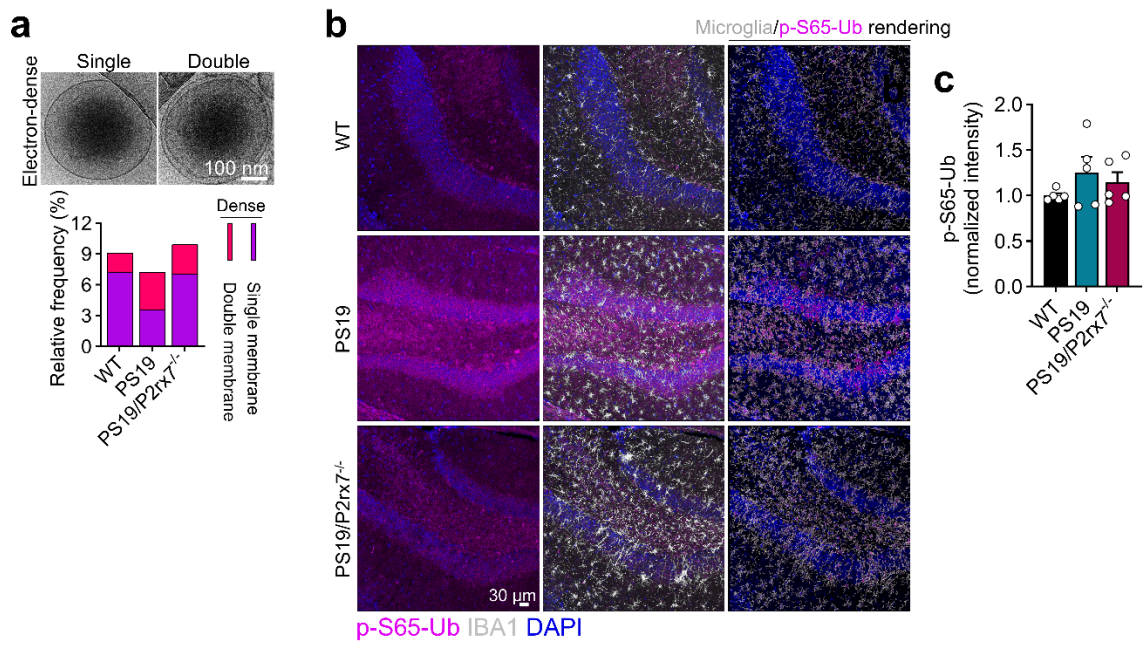

Extended Data Fig. 8: *P2rx7* deficiency effects on mitochondrial-derived electron-dense vesicles and mitophagy in PS19 mice. a, Cryo-EM analysis of percentage of single and double membrane electron-dense vesicles from total BDEVs population (*n*=3 mice per group; total BDEVs analyzed *n*= 110 WT, *n*= 166 PS19 and *n*= 141 PS19/P2rx7$^{-/-}$). **b**, Representative confocal images and 3D rendering of microglial IBA1 and p-S65-Ub staining in DG hippocampus area. **c,** Total p-S65-Ub intensity measures using Imaris (*n*= 5 WT mice, *n*= 5 PS19 mice, *n*= 5 PS19/P2rx7$^{-/-}$ mice; one-way ANOVA with Holm–Šidák post hoc analysis). All the bar graphs are represented by mean ± SEM; $^{**}P < 0.01$.

Supplementary information

Supplementary Fig. 1. Uncropped images for immunoblots associated with Fig. 7 c.

Supplementary Fig. 2. Figure exemplifying the gating strategy for mouse microglia fluorescence-activated cell sorting.

Supplementary Table 1. Hippocampus bulk RNA-seq.

Supplementary Table 2. scRNA-seq of brain cell clusters PS19 vs WT mice.

Supplementary Table 3. scRNA-seq of brain cell clusters PS19_P2rx7KO vs PS19 mice.

Supplementary Table 4. scRNA-seq of glial cells commom DEGs PS19_P2rx7KO vs PS19 mice.

Supplementary Table 5. scRNA-seq of microglia PS19 vs WT mice.

Supplementary Table 6. scRNA-seq of microglia subclusters (main genes) vs all other clusters.

Supplementary Table 7. scRNA-seq of microglia subclusters PS19_P2rx7KO vs PS19 mice.

Supplementary Table 8. Brain-EV proteomics.

Supplementary Table 9. RNA-seq of sorted microglia from EV-injected mice.